Dinitrogen cleavage and hydrogenation to ammonia with a uranium complex

Xiaoqing Xin, Iskander Douair, Yue Zhao, Shuao Wang, Laurent Maron, Congqing Zhu

Dinitrogen Cleavage and Hydrogenation to Ammonia with a Uranium Complex

Laurent Maron (laurent.maron@irsamc.ups-tlse.fr)
University of Toulouse https://orcid.org/0000-0003-2653-8557
Xiaoqing Xin
Nanjing University
Iskander Douair
Université de Toulouse et CNRS https://orcid.org/0000-0002-7482-5510
Shuao Wang
State Key Laboratory of Radiation Medicine and Protection, Soochow University
https://orcid.org/0000-0002-1526-1102
Congqing Zhu
Nanjing University https://orcid.org/0000-0003-4722-0484
Yue Zhao
https://orcid.org/0000-0001-6094-4087

Article

Keywords: Haber-Bosch process, dinitrogen cleavage, hydrogenation

Posted Date: September 30th, 2021

DOI: https://doi.org/10.21203/rs.3.rs-846715/v1

Abstract

The Haber–Bosch process produces ammonia (NH_3) from dinitrogen (N_2) and dihydrogen (H_2), but requires high temperature and pressure. Before iron-based catalysts were exploited in the current industrial Haber–Bosch process, uranium-based materials were used as effective catalysts for production of NH_3 from N_2. Although some molecular uranium complexes are capable of combining and even reducing N_2, however, further hydrogenation with H_2 to NH_3 has not yet been reported. Here, we report the first example of N_2 cleavage and hydrogenation with H_2 to NH_3 with a molecular uranium complex. The N_2 cleavage product contains three uranium centers that are bridged by three imido μ_2-NH ligands and one nitrido μ_3-N ligand. Labeling experiments with ^{15}N demonstrate that the nitrido ligand in the product originates from N_2. Reaction of the N_2-cleaved complex with H_2 or H^+ forms NH_3 under mild conditions. A synthetic cycle has been established by the reaction of the N_2-cleaved complex with TMSCl. The isolation of this trinuclear imido-nitrido product implies that a multimetallic uranium assembly plays an important role in the activation of N_2.

Background

Fixation, activation and functionalization of dinitrogen (N_2) are challenging issues in chemistry due to the presence of the unreactive and nonpolar N≡N triple bond in N_2.[i][ii][iii][iv][v][vi] Both nitrogenase enzymes and the industrial Haber-Bosch process for N_2 fixation use transition metals to catalyze this challenging transformation[vii],[viii] and thus catalytic N_2 fixation by transition metals and subsequent protonation to ammonia (NH_3) have been extensively studied in recent decades.[ix][x][xi] [xii][xiii][xiv][xv][xvi][xvii][xviii][xix][xx][xxi][xxii][xxiii][xxiv][xxv][xxvi] [xxvii][xxviii][xxix] However, examples of the direct hydrogenation of N_2-activated products with hydrogen (H_2) to form NH_3, similar to the industrial Haber–Bosch process, remain extremely uncommon.[12,16,29] Chirik and co-workers found that an N_2-derived Zr nitride complex could react with H_2 at 85 ^oC to give NH_3 in 10-15% yield (Fig. 1a).[12] Holland and co-workers reported an example of N_2 reduction and hydrogenation, forming NH_3 in 42% yield by a molecular iron-potassium species (Fig. 1b).[16] Recently, Walter and co-workers found that the NH_3 was formed in 3-7% yield from N_2 and H_2 mediated by a molecular tri-iron species (Fig. 1c).[29] These studies have led us to attempt to understand the Haber–Bosch process at the molecular level.

Although uranium-based materials were known to be effective catalysts for NH_3 production from N_2 before use of the iron-based catalysts in the current industrial Haber–Bosch process,[xxx] only few examples of well-defined uranium species capable of transforming N_2 into NH_3 were known for more than a century and all NH_3 formation processes required protonation with acid.[xxxi][xxxii][xxxiii][xxxiv] For instance, Mazzanti and co-workers reported a multimetallic nitride-bridged diuranium(III) complex, $[K_3\{[U(OSi(O^tBu)_3)_3]_2(\mu\text{-}N)\}]$, which can convert N_2 to NH_3 after protonation with acid.[31] Arnold *et al.*

recently reported thorium or uranium dinuclear metallacycles $M_2(m\text{TP})_2$ (M = U, Th; *m*TP = [{2-(OC_6H_2-^{t}Bu-2,Me-4)$_2$CH}-C_6H_4-1,3]$^{4-}$) which can mediate the reduction and protonation of N_2 to NH_3 in the presence of potassium graphite (KC_8).[32] However, examples of the hydrogenation of an N_2-activated product with H_2 to NH_3 by a molecular uranium complex have not yet been reported.

Herein we report the first example of NH_3 formation from the hydrogenation of an N_2-cleaved complex with H_2 in a molecular uranium system (Fig. 1d). The N_2-cleaved product was formed by the reduction of a uranium azide species with KC_8. The conversion of the N_2-cleaved product to silylamine was also achieved, thus a synthetic cycle has been established with the generation of the uranium precursor.

[i]. Schlögl, R. *Ammonia Synthesis, in Handbook of Homogeneous Catalysis*, Ertl, G., Knözinger, H., Schüth, F., Weitkamp, J. Eds. (Wiley, 2008).
[ii]. MacKay, B. A. & Fryzuk, M. D. Dinitrogen coordination chemistry: on the biomimetic borderlands. *Chem. Rev.* **104**, 385–402 (2004).
[iii]. Burford, R. J. & Fryzuk, M. D. Examining the relationship between coordination mode and reactivity of dinitrogen. *Nat. Rev. Chem.* **1**, 0026 (2017).
[iv]. Foster, S. L. *et al.* Catalysts for nitrogen reduction to ammonia. *Nat. Catal.* **1**, 490–500 (2018).
[v]. Légaré, M.-A. *et al*. Nitrogen fixation and reduction at boron. *Science* **359**, 896–900 (2018).
[vi]. Légaré, M.-A. *et al.* The reductive coupling of dinitrogen. *Science* **363**, 1329–1332 (2019).
[vii]. Einsle, O. *et al.* Nitrogenase MoFe-protein at 1.16 Å resolution: a central ligand in the FeMo-cofactor. *Science* **297,** 1696–1700 (2002).
[viii]. Hoffman, B. M., Lukoyanov, D., Yang, Z. Y., Dean, D. R. & Seefeldt, L. C. Mechanism of nitrogen fixation by nitrogenase: the next stage. *Chem. Rev.* **114**, 4041–4062 (2014).
[ix]. Laplaza, C. E. & Cummins, C. C. Dinitrogen cleavage by a three-coordinate molybdenum(III) complex. *Science* **268**, 861–863 (1995).
[x]. Yandulov, D. V. & Schrock, R. R. Catalytic reduction of dinitrogen to ammonia at a single molybdenum center. *Science* **301**, 76–78 (2003).
[xi]. Betley, T. A. & Peters, J. C. Dinitrogen chemistry from trigonally coordinated iron and cobalt platforms. *J. Am. Chem. Soc.* **125**, 10782–10783 (2003).
[xii]. Pool, J. A., Lobkovsky, E. & Chirik, P. J. Hydrogenation and cleavage of dinitrogen to ammonia with a zirconium complex. *Nature* **427**, 527–530 (2004).
[xiii]. Schrock, R. R. Catalytic reduction of dinitrogen to ammonia by molybdenum: theory versus experiment. *Angew. Chem. Int. Ed.* **47**, 5512–5522 (2008).
[xiv]. Knobloch, D. J., Lobkovsky, E. & Chirik, P. J. Dinitrogen cleavage and functionalization by carbon monoxide promoted by a hafnium complex. *Nat. Chem.* **2**, 30–35 (2010).
[xv]. Arashiba, K., Miyake, Y. & Nishibayashi, Y. A molybdenum complex bearing PNP-type pincer ligands leads to the catalytic reduction of dinitrogen into ammonia. *Nat. Chem.* **3**, 120–125 (2011).
[xvi]. Rodriguez, M. M., Bill, E., Brennessel, W. W. & Holland, P. L. N_2 reduction and hydrogenation to ammonia by a molecular iron-potassium complex. *Science* **334**, 780–783 (2011).

[xvii]. MacLeod, K. C. & Holland, P. L. Recent developments in the homogeneous reduction of dinitrogen by molybdenum and iron. *Nat. Chem.* **5**, 559–565 (2013).
[xviii]. Anderson, J. S., Rittle, J. & Peters, J. C. Catalytic conversion of nitrogen to ammonia by an iron model complex. *Nature* **501**, 84–87 (2013).
[xix]. Shima, T. *et al.* Dinitrogen cleavage and hydrogenation by a trinuclear titanium polyhydride complex. *Science* **340**, 1549–1552 (2013).
[xx]. Čorić, I., Mercado, B. Q., Bill, E., Vinyard, D. J. & Holland, P. L. Binding of dinitrogen to an iron–sulfur–carbon site. *Nature* **526**, 96–99 (2015).
[xxi]. Tanaka, H., Nishibayashi, Y. & Yoshizawa, K. Interplay between theory and experiment for ammonia synthesis catalyzed by transition metal complexes. *Acc. Chem. Res.* **49**, 987–995 (2016).
[xxii]. Silantyev, G. A. *et al.* Dinitrogen splitting coupled to protonation. *Angew. Chem. Int. Ed.* **56**, 5872–5876 (2017).
[xxiii]. Gao, Y., Li, G. & Deng, L. Bis(dinitrogen)cobalt(−1) complexes with NHC ligation: Synthesis, characterization, and their dinitrogen functionalization reactions affording side-on bound diazene complexes. *J. Am. Chem. Soc.* **140**, 2239–2250 (2018).
[xxiv]. Geng, C., Li, J., Weiske, T. & Schwarz, H. Ta_2^+-mediated ammonia synthesis from N_2 and H_2 at ambient temperature. *Proc. Natl. Acad. Sci. U. S. A.* **115**, 11680-11687 (2018).
[xxv]. Ashida, Y., Arashiba, K., Nakajima, K. & Nishibayashi, Y. Molybdenum-catalysed ammonia production with samarium diiodide and alcohols or water. *Nature* **568**, 536-540 (2019).
[xxvi]. Lv, Z.-J., Huang, Z., Zhang, W.-X. & Xi, Z. Scandium-promoted direct conversion of dinitrogen into hydrazine derivatives via N–C bond formation. *J. Am. Chem. Soc.* **141**, 8773–8777 (2019).
[xxvii]. Yin, J. *et al.* Dinitrogen functionalization affording chromium hydrazido complex. *J. Am. Chem. Soc.* **141**, 4241–4247 (2019).
[xxviii]. Lv, Z.-J. *et al.* Direct transformation of dinitrogen: synthesis of N-containing organic compounds via N–C bond formation. *Natl. Sci. Rev.* **7**, 1564–1583 (2020).
[xxix]. Reiners, M. *et al.* NH_3 formation from N_2 and H_2 mediated by molecular tri-iron complexes. *Nat. Chem.* **12**, 740–746 (2020).
[xxx] Haber, F. Verfahren zur Herstellung von Ammoniak durch katalytische Vereinigung von Stickstoff und Wasserstoff, zweckmäßig unter hohem Druch. *German patent DE* 229126 (1909).
[xxxi]. Falcone, M., Chatelain, L., Scopelliti, R., Živković, I. & Mazzanti, M. Nitrogen reduction and functionalization by a multimetallic uranium nitride complex. *Nature* **547**, 332–335 (2017).
[xxxii]. Arnold, P. L. *et al.* Metallacyclic actinide catalysts for dinitrogen conversion to ammonia and secondary amines. *Nat. Chem.* **12**, 654–659 (2020).
[xxxiii]. Xin, X. *et al.* Dinitrogen cleavage by a multimetallic cluster featuring uranium–rhodium bond. *J. Am. Chem. Soc.* **142**, 15004-15011 (2020).
[xxxiv]. Wang, P. *et al.* Facile dinitrogen and dioxygen cleavage by a uranium(III) complex: cooperativity between the non-innocent ligand and the uranium center. *Angew. Chem. Int. Ed. 60*, 473–479 (2021).

Results

Synthesis, characterization, and transformation. Treatment of the complex {U[N(CH_3)($CH_2CH_2NP^iPr_2$)$_2$]$(Cl)_2$(THF)} (**1**)[33] with 2 equiv. of NaN_3 at room temperature (RT) in tetrahydrofuran (THF) results in the formation of a molecular chain, [{[U{N(CH_3)($CH_2CH_2NP^iPr_2$)$_2$}(N_3)](μ-N_3)}$_n$] (**2**), which was isolated in 72% yield as a crystalline product (Fig. 1d). The ^{1}H NMR spectrum of **2** has eleven peaks between + 69.64 and − 70.48 ppm (Fig. S1), indicating an unsymmetrical structure. The Fourier-transform infrared (FT-IR) spectrum of **2** exhibits two strong azide stretching bands at 2094 cm^{-1} and 2150 cm^{-1} (Fig. S2), which are characteristic of actinide-bound terminal and bridged azide ligands, respectively.[-]

The molecular structure of complex **2** was confirmed by single-crystal X-ray diffraction, which exhibits a novel one-dimensional molecular chain connected through 1,3-end-on bridged azides (Fig. 2a). The U–N_{azide} distances between the uranium and bridged azide are 2.447(3) Å for U1-N3 and 2.471(4) Å for U1'-N1, which are clearly longer than the terminal U–N_{azide} distance (U1–N6 2.292(3) Å) but are similar to those found in previously reported multimetallic uranium complexes with bridged azide ligands.[36,,] The N1–N2 and N2–N3 bond lengths are 1.159(4) and 1.169(4) Å, respectively, suggesting that a delocalized$^-$N = N$^+$=N$^-$ resonance form is predominant in this 1,3-end-on bridged azide. However, the terminal azide shows a more localized form with N4–N5 and N5–N6 bond lengths of 1.145(5) and 1.181(5) Å, respectively, suggesting weak activation of this terminal azide.

Uranium azides are well-known as synthetic precursors of terminal uranium nitride species in photochemical or redox processes.[35,36,,] We first investigated the photolysis or thermolysis of complex **2**, but the products were unidentifiable. However, when complex **2** was reduced with an excess of KC_8 in a toluene-THF mixed solvent under an N_2 atmosphere, the color of the solution changed immediately from yellow-brown to dark-brown (Fig. 1d). Upon work-up of this mixture, a crystalline complex, [{[U{N(CH_3)($CH_2CH_2NP^iPr_2$)$_2$}(μ-NH)]$_3$(μ-N)}K_2] (**3**) was isolated in 31% yield. The ^{1}H NMR spectrum of **3** exhibits paramagnetic resonance signals between + 73.69 and − 33.22 ppm (Fig. S4). Complex **3** could also be prepared by the reduction of **2** with KC_8 under Ar, albeit with a lower crystalline yield (16%). Attempts to increase the yield of complex **3** were unsuccessful although it was the major product in the *in-situ* reaction of complex **2** with KC_8 (Fig. S5). Toluene dimers were detected by gas chromatography-mass spectrometric (GC-MS) analysis of the reaction mixture (Fig. S6), which is consistent with the failure to obtain complex **3** when the reaction was conducted in the absence of toluene. Complex **3** could be also formed by the reaction of complex **2** with an excess of KC_8 in THF in the presence of 9,10-dihydroanthracene (Fig. S7). These results suggest that the proton source plays an important role in the formation of **3**. The presence of N-H groups in **3** was confirmed by the formation of $HN(SiMe_3)_2$ in the reaction of **3** with TMSCl (*vide infra*) and the broad absorption at 3450 cm^{-1} in the FT-IR spectrum of complex **3** (Fig. S3) .[35,36]

The molecular structure of complex **3** was confirmed by X-ray crystallography (Fig. 2b). The salient feature of this structure is the presence of three U centers bridged by three imido μ-NH ligands and one nitrido μ_3-N ligand. The six U–N_{imido} bond lengths fall in the range of 2.188 − 2.231 Å and are comparable

with the bridged U–N_{imido} distances reported previously in the range of 2.10–2.55 Å.[32,,] These near-equivalent U–N_{imido} bond lengths suggest that it is not a U–N = U bonding interaction but a U–NH–U unit by the comparison with reported analogues.[44,] The three U-$N_{nitrido}$ distances which range from 2.204 to 2.218 Å are comparable to those found in U(IV)/U(VI) tetrauranium nitride clusters (2.183(7)-2.319(78) Å) and slightly longer than those found in a μ_3-N nitride uranium complex (2.138–2.157 Å). Despite their bridging nature, the U-N_{imido} and U-$N_{nitrido}$ bond lengths in **3** remain slightly shorter than the sum of the single bond covalent radii of U and N (2.41 Å). Although similar trinuclear imido-nitride structures with transition metals have been described by the groups of Roesky, Yélamos, and Hou,[19] complex **3** represents the first example of a trinuclear uranium species with both imido and nitrido ligands.

To verify the source of the nitrido ligand in complex **3**, we reduced complex **2** with KC_8 under 1 atm of $^{15}N_2$. After the acidification of the ^{15}N-labelled product (**3-^{15}N**) with excess pyridine hydrochloride, a triplet resonance (δ = 7.42 ppm, J_{NH} = 52 Hz, assigned to NH_4Cl) and a doublet resonance (δ = 7.42 ppm, J_{NH} = 72 Hz, assigned to $^{15}NH_4Cl$) were observed in a ratio of approximately 3:0.5 in its ^{1}H NMR spectrum in deuterated dimethyl sulfoxide (Fig. S12). Exposing the THF solution of complex **3** to 1 atm $^{15}N_2$ for 2 days does not reveal any exchange between **3** and $^{15}N_2$ (Fig. S13). Thus the generation of $^{15}NH_4Cl$ reveals that the $^{15}N_2$ cleavage was involved in the formation of complex **3**. The lower ratio of $^{15}NH_4Cl$ (the ideal ratio for $^{14}NH_4^+$:$^{15}NH_4^+$ is 3:1) is presumably because three molecules of $^{14}N_2$ are generated from the reduction of U-N_3 even under the $^{15}N_2$ conditions. This result is consistent with the isolation of complex **3** with lower yield when the reduction of complex **2** took place under an Ar atmosphere, in which the N_2 was generated *in-situ* by the reduction of N_3^- units. Furthermore, the *in-situ* ^{1}H NMR spectrum for the reaction of **2** with KC_8 under dynamic vacuum reveals that no complex **3** was formed (Fig. S14). These studies demonstrate that the nitrido ligand in complex **3** originates from N_2. Fixing and activation of N_2 derived from the reduction of metal azides is very rare for either *d*- or *f*-block metals. Liddle and co-workers isolated a uranium(v)–bis(imido)–dinitrogen complex, [U(BIPM^{TMS})(NAd)$_2$(μ-η^1:η^1-N_2)(Li-2,2,2-cryptand)], by reacting a uranium-carbene species with an organoazide under an N_2 or Ar atmosphere. The N-N length of the coordinated N_2 in this species (1.139(9) Å) is only slightly elongated over the N-N length in the free N_2 molecule (1.0975 Å). Therefore, complex **3** represents the first example of N_2 scission in a metal-azide reduction.

Direct hydrogenation of the N_2-activated product with H_2 under mild conditions is desirable. Accordingly, complex **3** was treated with H_2 at atmospheric pressure and RT (Fig. 1d). The *in-situ* ^{1}H NMR and ^{31}P{^{1}H} NMR spectra show that complex **3** was consumed within 8 h and the free ligand was formed in the reaction (Figs. S15 and S16). The formation of NH_3 in 34% yield was identified by the formation of NH_4Cl after treating the volatiles with an excess of PyHCl (Fig. S17). The NH_3 formation in this hydrogenation process was further confirmed by the reaction of complex **3** with 1 atm D_2 at RT, which affords ND_3 as confirmed by the ^{2}H NMR spectrum (Fig. S18). This process represents the first example of NH_3

production by the hydrogenation of an N_2-activated product with H_2 or D_2 in a uranium system. The reaction of ^{15}N-labelled product (**3-^{15}N**) with H_2 generates NH_3 and $^{15}NH_3$ (Fig. S19), which shows that the imido and nitrido groups in complex **3** were converted to NH_3. In addition, by the reaction of complex **3** with an excess of Me_3SiCl (TMSCl) at RT for overnight, the uranium precursor (complex **1**, 46% yield) and N-containing products ($HN(SiMe_3)_2$ and $N(SiMe_3)_3$) were formed (Figs. S20 and S21). Therefore, a synthetic cycle has been established and the uranium-containing precursor can be reused (Fig. 1d).

The oxidation state of the uranium center in complex **2** is + IV, which was confirmed by the variable-temperature magnetic data determined by a super-conducting quantum interference device (SQUID) in the solid state (Fig. 3). The magnetic moment of complex **2** is 3.37 μ_B at 300 K and smoothly decreases to 0.45 μ_B at 1.8 K, then approaches zero (Fig. 3a). The magnitude of μ_{eff} and temperature dependence of **2** are consistent with a U(IV) center which is a magnetic singlet at low temperatures.[36,41,-] Formally, complex **3** contains two U(IV) centers and one U(V) center. The measured magnetic moment at 300 K for complex **3**, which contains three U ions, is 5.72 μ_B, and also exhibits significant temperature dependence decreasing steadily to 1.39 μ_B at 1.8 K (Fig. 3b). The UV-Visible-NIR absorption spectra of complexes **2** and **3** were recorded in THF at RT (Fig. S24). Complex **2** displays moderate absorption in the 300–450 nm range, while **3** exhibits a significantly more intense absorption than that of **2** over the entire visible and NIR region. Both **2** and **3** exhibit several weak absorption peaks ($\varepsilon < 50$ and 200 M^{-1} cm^{-1} for **2** and **3**, respectively) in the NIR region, which is characteristic of *f-f* transitions involving the $5f^1$ and $5f^2$ electronic configuration.[52,-] X-ray photoelectron spectroscopy (XPS) was undertaken to investigate the probable oxidation state of uranium in complex **3** (Fig. S25). The binding energy for U-4$f_{7/2}$ in the XPS of **3** was observed to be 380.52 eV, which is in the range of the binding energies for U(IV) and U(V) species.[-] These results are consistent with the assignment of U(IV)/U(IV)/U(V) to complex **3** and the overall charge of this cluster was balanced with two K^+ ions.

The formation of imido ligand in complex **3** is proposed to involve a terminal uranium nitride, which was formed by the reduction of uranium azide **2** with KC_8 and followed by protonation to the imido ligand by toluene or 9.10-dihydroanthracene. Attempts to isolate this terminal uranium nitride intermediate at low temperatures and/or with diminished levels of KC_8 were unsuccessful. Reduction and oligomerization of metal azides induced by photolysis or thermolysis are quite common, but the observed subsequent cleavage of the N ≡ N triple bond in N_2 is a hitherto unknown process for either *d*- or *f*-block elements.

Theoretical studies. To further investigate the conversion of **1** to **3**, density functional theory (DFT) calculations were carried out using the B3PW91 functional that have been proved to be reliable in dealing with such systems.[32–34] Dispersion corrections were considered and appeared to be small in this case (Figs. S28 and S29). The Gibbs free energies were reported and the difference with the enthalpy barriers was only 1.0 kcal mol^{-1}.

Experimentally, complex **2** is a coordination polymer that could not be computationally modeled. However, the formation of a monomer (**2'**) was predicted to be favorable by 17.0 kcal mol^{-1} (Fig. 4). The main geometrical features of **2** were correctly reproduced in the computed monomeric form **2'**. For instance, the U-N distances are 2.26 Å vs. 2.24 Å (exp) and the N-N distances are 1.21/1.15 Å vs. 1.18/1.15 Å (exp.). The unpaired spin density is 2.166, consistent with a U(IV) center. Reduction of the diazide **2'** is predicted to be almost athermic (0.8 kcal mol^{-1}) and is assisted by the coordination of a K^+ to form a monoazide complex **A**.[36,42] In the absence of potassium coordination, the reduction is endothermic by 28.6 kcal mol^{-1} (Fig. S29). The reduction of the U(IV) center is highlighted by the unpaired spin density value of 3.12 at the uranium center of **A**, which is consistent with a U(III) system. This monoazide complex **A** stabilized by a potassium cation can further evolve to a nitride complex **B** by losing N_2. A potassium-mediated N_2-release transition state (**TS1**) has been located and the associated barrier is 15.5 kcal mol^{-1}, in line with a facile process.

The significance of the potassium is evidenced by two facts. First, the release of N_2 from the monomeric form of **2'** in the absence of K was calculated to imply an activation barrier of 46.7 kcal mol^{-1} (28.6 kcal mol^{-1} from the uncapped monoazide complex, Fig. S29). Interestingly, the N-N bond cleavage implies a single electron transfer from the uranium center to the azide ligand. Indeed, at the **TS1**, the unpaired spin density appears to be distributed between U (2.193), in line with a U(IV) system, and the two terminal nitrogen atoms of the azide ligand (0.541 for the nitride and 0.415 for the N_2), that are stabilized by the potassium cation. Following the intrinsic reaction coordinate, **TS1** releases N_2, forming a nitrido-type intermediate **B**, whose formation from the diazide complex **2'** is slightly endothermic by 3.2 kcal mol^{-1} (Fig. 4). Intermediate **B** is better described as a U(IV)-(nitride radical)-K(I) complex since the unpaired spin density is distributed between U (2.254) and N (0.700). The presence of an unpaired electron at the nitride indicateds that this intermediate is fairly unstable and will react further with potassium to yield a dianionic uranium-nitride (**C**) stabilized by two potassium counterions (-66.3 kcal mol^{-1} from **1**, -49.3 kcal mol^{-1} from the diazide **2'**). The intermediate **C** is also interesting because the unpaired spin density indicates that the potassium does not reduce the metal but reduces the nitride, yielding a U(IV)-N(-III)-2K(I) species (unpaired spin density of 2.125 on U, and 0.607 and 0.426 on the two K ions).

Intermediate **C** is therefore sufficiently nucleophilic to abstract a hydrogen from the solvent. The relevant **TS2** was located and the associated barrier is 9.4 kcal mol^{-1} indicating a facile reaction (Fig. 5). The charge on the hydrogen (+ 0.22) shows that this reaction is a proton transfer rather than a hydrogen atom transfer reaction (HAT) and this is possibly due to the presence of a U(IV)-N(-III) unit in **C**. At the **TS2**, the assistance from the potassium is again crucial since an observed interaction between one potassium and the phenyl ring of the toluene, allows the proton transfer. Following the intrinsic reaction coordinate, this leads to the formation of a $PhCH_2K$ adduct to the U(IV)-imido complex **D** (-85.2 kcal mol^{-1} from the entrance channel), which can easily trimerize while losing $PhCH_2K$ to form complex **E** (-119.1 kcal mol^{-1}). The trimetallic tri-imido species **E** can then bind N_2 to form **F** (-113.3 kcal mol^{-1}). In **F**, the three uranium centers are U(IV) (unpaired spin densities of ~ 2.17 per U) and the N_2 is not reduced (N-N bond distance of

1.19 Å) but binds to the uranium (U-N_2 WBI of 0.26). Interestingly, the LUMO of **F** is a bonding interaction between the uranium centers and the π* of N_2 (Fig. S30).

Finally, reduction of **F** yields species **G** (-103.4 kcal mol^{-1}), in which the N_2 moiety is triply reduced and has an N-N bond distance of 1.3 Å with an unpaired spin density of 0.8 on N_2. This implies that one uranium center has been oxidized, as evidenced by the unpaired spin densities of U (Fig. 5). Complex **G** is thus half-way to complex **3**, and **3** is formed upon coordination of a second complex **E**. The formation of **3** from **1** is exothermic by -131.2 kcal mol^{-1}. The optimized geometry of **3** compares well with the experimental observations. The U-N bond distances for example are correctly reproduced (between 2.17 and 2.24 Å vs. between 2.17 and 2.23 Å exp.). Scrutiny of the unpaired spin density in **3** allows determination of two U(IV) and one U(V) in this species (Fig. 6). Upon comparison of the uranium oxidation states found for the nitride and imido complexes, the formation of **3** implies a N ≡ N bond cleavage *via* trimetallic uranium synergy, but only a single electron oxidation of one uranium center, which is surprising at first glance. However, the other electrons used for the reduction are stored in the potassium.

Conclusion

In summary, we are reporting the first example of N_2 cleavage and hydrogenation with H_2 to NH_3 in a uranium system. The N_2-cleaved product was formed by the reduction of a uranium azide complex, which has not been observed previously for the reduction of any *d*-block or *f*-block metal azides. The detailed mechanism of N_2 activation by multimetallic synergy was revealed by DFT calculations, which shows that the formation of **3** from **1** is likely to involve the formation of a transient U(IV)-nitride and U(IV)-imido complexes. The reduction of N_2 yields the final trinuclear imido-nitrido uranium complex, which can be protonated by H_2 or H^+ to NH_3 under mild conditions. The uranium precursor **1** was generated by the functionalization of **3** with TMSCl, thereby establishing a synthetic cycle. This study suggests that multiple uranium atoms can cooperate in the cleavage of N ≡ N triple bond in N_2 and that uranium species are promising materials for activation and conversion of small molecule.

Methods

General considerations. Experiments were performed under an Ar or N_2 atmosphere using standard Schlenk-line or glove-box techniques. Solvents were dried and degassed with a solvent purification system before use. See the Supplementary Information for detailed experimental procedures, crystallographic, and computational details.

Data Availability. The X-ray crystallographic coordinates for structures reported in this study have been deposited at the Cambridge Crystallographic Data Centre (CCDC), under deposition numbers CCDC-2021046 (**2**), 2021047 (**3**, prepared under Ar) and 2044515 (**3**, prepared under N_2). These data can be

obtained free of charge from the CCDC *via* www.ccdc.cam.ac.uk/data_request/cif. The data that support the findings of this study are available from the corresponding author upon reasonable request.

Declarations

Acknowledgements

This research was supported by the National Natural Science Foundation of China (Grant Nos. 21772088 and 91961116), the Fundamental Research Funds for the Central Universities (14380216), Programs for high-level entrepreneurial and innovative talents introduction of Jiangsu Province (individual and group programs). LM is member of the Institute Universitaire de France. Humboldt Foundation and Chinese Academy of Science are acknowledged for support. CalMip is also gratefully acknowledged for a generous grant of computing time.

Author contributions

C.Z. conceived this project. X.X. performed the experiments and solved all the X-ray structures with support from Y.Z. C.Z. and X.X. analyzed the experimental data. I.D. and L.M. conducted the theoretical calculations. L.M. analyzed the theoretical results. C.Z. and L.M. drafted the paper with support from others. All authors discussed the results and contributed to the preparation of the final manuscript.

Additional information

Supplementary Information accompanies this paper at http://www.nature.com/

naturechemistry.

Competing interests: The authors declare no competing interests.

Reprints and permission information is available online at http://npg.nature.com/

reprintsandpermissions/

References

1. Schlögl, R. *Ammonia Synthesis, in Handbook of Homogeneous Catalysis*, Ertl, G., Knözinger, H., Schüth, F., Weitkamp, J. Eds. (Wiley, 2008).
2. MacKay, B. A. & Fryzuk, M. D. Dinitrogen coordination chemistry: on the biomimetic borderlands. *Chem. Rev.* **104**, 385–402 (2004).
3. Burford, R. J. & Fryzuk, M. D. Examining the relationship between coordination mode and reactivity of dinitrogen. *Nat. Rev. Chem.* **1**, 0026 (2017).
4. Foster, S. L. *et al.* Catalysts for nitrogen reduction to ammonia. *Nat. Catal.* **1**, 490–500 (2018).
5. Légaré, M.-A. *et al*. Nitrogen fixation and reduction at boron. *Science* **359**, 896–900 (2018).

6. Légaré, M.-A. *et al.* The reductive coupling of dinitrogen. *Science* **363**, 1329–1332 (2019).
7. Einsle, O. *et al.* Nitrogenase MoFe-protein at 1.16 Å resolution: a central ligand in the FeMo-cofactor. *Science* **297,** 1696–1700 (2002).
8. Hoffman, B. M., Lukoyanov, D., Yang, Z. Y., Dean, D. R. & Seefeldt, L. C. Mechanism of nitrogen fixation by nitrogenase: the next stage. *Chem. Rev.* **114**, 4041–4062 (2014).
9. Laplaza, C. E. & Cummins, C. C. Dinitrogen cleavage by a three-coordinate molybdenum(III) complex. *Science* **268**, 861–863 (1995).
10. Yandulov, D. V. & Schrock, R. R. Catalytic reduction of dinitrogen to ammonia at a single molybdenum center. *Science* **301**, 76–78 (2003).
11. Betley, T. A. & Peters, J. C. Dinitrogen chemistry from trigonally coordinated iron and cobalt platforms. *J. Am. Chem. Soc.* **125**, 10782–10783 (2003).
12. Pool, J. A., Lobkovsky, E. & Chirik, P. J. Hydrogenation and cleavage of dinitrogen to ammonia with a zirconium complex. *Nature* **427**, 527–530 (2004).
13. Schrock, R. R. Catalytic reduction of dinitrogen to ammonia by molybdenum: theory versus experiment. *Angew. Chem. Int. Ed.* **47**, 5512–5522 (2008).
14. Knobloch, D. J., Lobkovsky, E. & Chirik, P. J. Dinitrogen cleavage and functionalization by carbon monoxide promoted by a hafnium complex. *Nat. Chem.* **2**, 30–35 (2010).
15. Arashiba, K., Miyake, Y. & Nishibayashi, Y. A molybdenum complex bearing PNP-type pincer ligands leads to the catalytic reduction of dinitrogen into ammonia. *Nat. Chem.* **3**, 120–125 (2011).
16. Rodriguez, M. M., Bill, E., Brennessel, W. W. & Holland, P. L. N_2 reduction and hydrogenation to ammonia by a molecular iron-potassium complex. *Science* **334**, 780–783 (2011).
17. MacLeod, K. C. & Holland, P. L. Recent developments in the homogeneous reduction of dinitrogen by molybdenum and iron. *Nat. Chem.* **5**, 559–565 (2013).
18. Anderson, J. S., Rittle, J. & Peters, J. C. Catalytic conversion of nitrogen to ammonia by an iron model complex. *Nature* **501**, 84–87 (2013).
19. Shima, T. *et al.* Dinitrogen cleavage and hydrogenation by a trinuclear titanium polyhydride complex. *Science* **340**, 1549–1552 (2013).
20. Čorić, I., Mercado, B. Q., Bill, E., Vinyard, D. J. & Holland, P. L. Binding of dinitrogen to an iron–sulfur–carbon site. *Nature* **526**, 96–99 (2015).
21. Tanaka, H., Nishibayashi, Y. & Yoshizawa, K. Interplay between theory and experiment for ammonia synthesis catalyzed by transition metal complexes. *Acc. Chem. Res.* **49**, 987–995 (2016).
22. Silantyev, G. A. *et al.* Dinitrogen splitting coupled to protonation. *Angew. Chem. Int. Ed.* **56**, 5872–5876 (2017).
23. Gao, Y., Li, G. & Deng, L. Bis(dinitrogen)cobalt(−1) complexes with NHC ligation: Synthesis, characterization, and their dinitrogen functionalization reactions affording side-on bound diazene complexes. *J. Am. Chem. Soc.* **140**, 2239–2250 (2018).

24. Geng, C., Li, J., Weiske, T. & Schwarz, H. Ta_2^+-mediated ammonia synthesis from N_2 and H_2 at ambient temperature. *Proc. Natl. Acad. Sci. U. S. A.* **115**, 11680-11687 (2018).
25. Ashida, Y., Arashiba, K., Nakajima, K. & Nishibayashi, Y. Molybdenum-catalysed ammonia production with samarium diiodide and alcohols or water. *Nature* **568**, 536-540 (2019).
26. Lv, Z.-J., Huang, Z., Zhang, W.-X. & Xi, Z. Scandium-promoted direct conversion of dinitrogen into hydrazine derivatives via N–C bond formation. *J. Am. Chem. Soc.* **141**, 8773–8777 (2019).
27. Yin, J. *et al.* Dinitrogen functionalization affording chromium hydrazido complex. *J. Am. Chem. Soc.* **141**, 4241–4247 (2019).
28. Lv, Z.-J. *et al.* Direct transformation of dinitrogen: synthesis of N-containing organic compounds via N–C bond formation. *Natl. Sci. Rev.* **7**, 1564–1583 (2020).
29. Reiners, M. *et al.* NH_3 formation from N_2 and H_2 mediated by molecular tri-iron complexes. *Nat. Chem.* **12**, 740–746 (2020).
30. Haber, F. Verfahren zur Herstellung von Ammoniak durch katalytische Vereinigung von Stickstoff und Wasserstoff, zweckmäßig unter hohem Druch. *German patent DE* 229126 (1909).
31. Falcone, M., Chatelain, L., Scopelliti, R., Živković, I. & Mazzanti, M. Nitrogen reduction and functionalization by a multimetallic uranium nitride complex. *Nature* **547**, 332–335 (2017).
32. Arnold, P. L. *et al.* Metallacyclic actinide catalysts for dinitrogen conversion to ammonia and secondary amines. *Nat. Chem.* **12**, 654–659 (2020).
33. Xin, X. *et al.* Dinitrogen cleavage by a multimetallic cluster featuring uranium–rhodium bond. *J. Am. Chem. Soc.* **142**, 15004-15011 (2020).
34. Wang, P. *et al.* Facile dinitrogen and dioxygen cleavage by a uranium(III) complex: cooperativity between the non-innocent ligand and the uranium center. *Angew. Chem. Int. Ed. 60*, 473–479 (2021).
35. Thomson, R. K. *et al.* Uranium azide photolysis results in C–H bond activation and provides evidence for a terminal uranium nitride. *Nat. Chem.* **2**, 723–729 (2010).
36. Du, J. *et al.* Thorium- and uranium-azide reductions: a transient dithorium-nitride versus isolable diuranium-nitrides. *Chem. Sci.* **10**, 3738–3745 (2019).
37. Haiges, R., Vasiliu, M., Dixon, D. A. & Christe, K. O. The uranium(VI) oxoazides $[UO_2(N_3)_2{\cdot}CH_3CN]$, $[(bipy)_2(UO_2)_2(N_3)_4]$, $[(bipy)UO_2(N_3)_3]^-$, $[UO_2(N_3)_4]^{2-}$, and $[(UO_2)_2(N_3)_8]^{4-}$. *Chem.-Eur. J.* **23**, 652–664 (2017).
38. Zhou, W., McKearney, D. & Leznoff, D. B. Structural diversity of f-element monophthalocyanine complexes. *Chem.-Eur. J.* **26**, 1027–1031 (2020).
39. Evans, W. J., Kozimor, S. A. & Ziller, J. W. Molecular octa-uranium rings with alternating nitride and azide bridges. *Science* **309**, 1835–1838 (2005).
40. Nocton, G., Pécaut, J. & Mazzanti, M. A nitride-centered uranium azido cluster obtained from a uranium azide. *Angew. Chem. Int. Ed.* **47**, 3040–3042 (2008).

41. King, D. M. *et al.* Isolation and characterization of a uranium(VI)–nitride triple bond. *Nat. Chem.* **5**, 482–488 (2013).
42. Mullane, K. C. *et al.* C–H bond addition across a transient uranium–nitrido moiety and formation of a parent uranium imido complex. *J. Am. Chem. Soc.* **140**, 11335–11340 (2018).
43. Falcone, M. *et al.* The role of bridging ligands in dinitrogen reduction and functionalization by uranium multimetallic complexes. *Nat. Chem.* **11**, 154–160 (2019).
44. Palumbo, C. T., Scopelliti, R., Zivkovic, I. & Mazzanti, M. C–H bond activation by an isolated dinuclear U(III)/U(IV) nitride. *J. Am. Chem. Soc.* **142**, 3149–3157 (2020).
45. Fortier, S.; Wu, G. & Hayton, T. W. Synthesis of a nitrido-substituted analogue of the uranyl ion, [N=U=O]+. *J. Am. Chem. Soc.* **132**, 6888–6889 (2010).
46. Jori, N. *et al.* Stepwise reduction of dinitrogen by a uranium–potassium complex yielding a U(VI)/U(IV) tetranitride cluster. *J. Am. Chem. Soc.* **143**, 11225–11234 (2021).
47. Evans, W. J., Miller, K. A., Ziller, J. W. & Greaves, J. Analysis of uranium azide and nitride complexes by atmospheric pressure chemical ionization mass spectrometry. *Inorg. Chem.* **46**, 8008–8018 (2007).
48. Pyykkö, P. & Atsumi, M. Molecular single-bond covalent radii for elements 1–118. *Chem.-Eur. J.* **15**, 186–197 (2009).
49. Roesky, H. W., Bai, Y. & Noltemeyer, M. Synthesis and structure of $[\{(\eta^5\text{-}C_5Me_5)Ti(NH)\}_3N]$, a titanium imide nitride. *Angew. Chem., Int. Ed. Engl.* **28**, 754–755 (1989).
50. Barriopedro, P., Caballo, J., Mena, M., Pérez-Redondo, A. & Yélamos, C. Successive protonation and methylation of bridging imido and nitrido ligands at titanium complexes. *Inorg. Chem.* **59**, 7631–7643 (2020).
51. Lu, E. *et al.* Back-bonding between an electron-poor, high-oxidation-state metal and poor π-acceptor ligand in a uranium(V)–dinitrogen complex. *Nat. Chem.* **11**, 806–811 (2019).
52. Castro-Rodriguez, I., Nakai, H., Zakharov, L. N., Rheingold, A. L. & Meyer, K. A linear, O-coordinated η^1-CO_2 bound to uranium. *Science* **305**, 1757–1759 (2004).
53. Liddle, S. T. The Renaissance of non-aqueous uranium chemistry. *Angew. Chem., Int. Ed.* **54**, 8604–8641 (2015).
54. Kindra, D. R. & Evans, W. J. Magnetic susceptibility of uranium complexes. *Chem. R*ev. **114**, 8865–8882 (2014).
55. Anderson, N. H. *et al.* Investigation of the electronic ground states for a reduced pyridine(diimine) uranium series: evidence for a ligand tetraanion stabilized by a uranium dimer. *J. Am. Chem. Soc.* **137**, 4690–4700 (2015).
56. Mills, D. P. *et al.* A delocalized arene-bridged diuranium single-molecule magnet. *Nat. Chem.* **3**, 454–460 (2011).
57. Schmidt, A.-C., Heinemann, F. W., Maron, L. & Meyer, K. A series of uranium (IV, V, VI) tritylimido complexes, their molecular and electronic structures and reactivity with CO_2. *Inorg. Chem.* **53**,

13142–13153 (2014).

58. Ilton, E. S. & Bagus, P. S. XPS determination of uranium oxidation states. *Surf. Interface Anal.* **43**, 1549–1560 (2011).
59. Bera, S., Sali, S. K., Sampath, S., Narasimhan, S. V. & Venugopal, V. Oxidation state of uranium: an XPS study of alkali and alkaline earth uranates. *J. Nucl. Mater.***255**, 26–33 (1998).

Figures

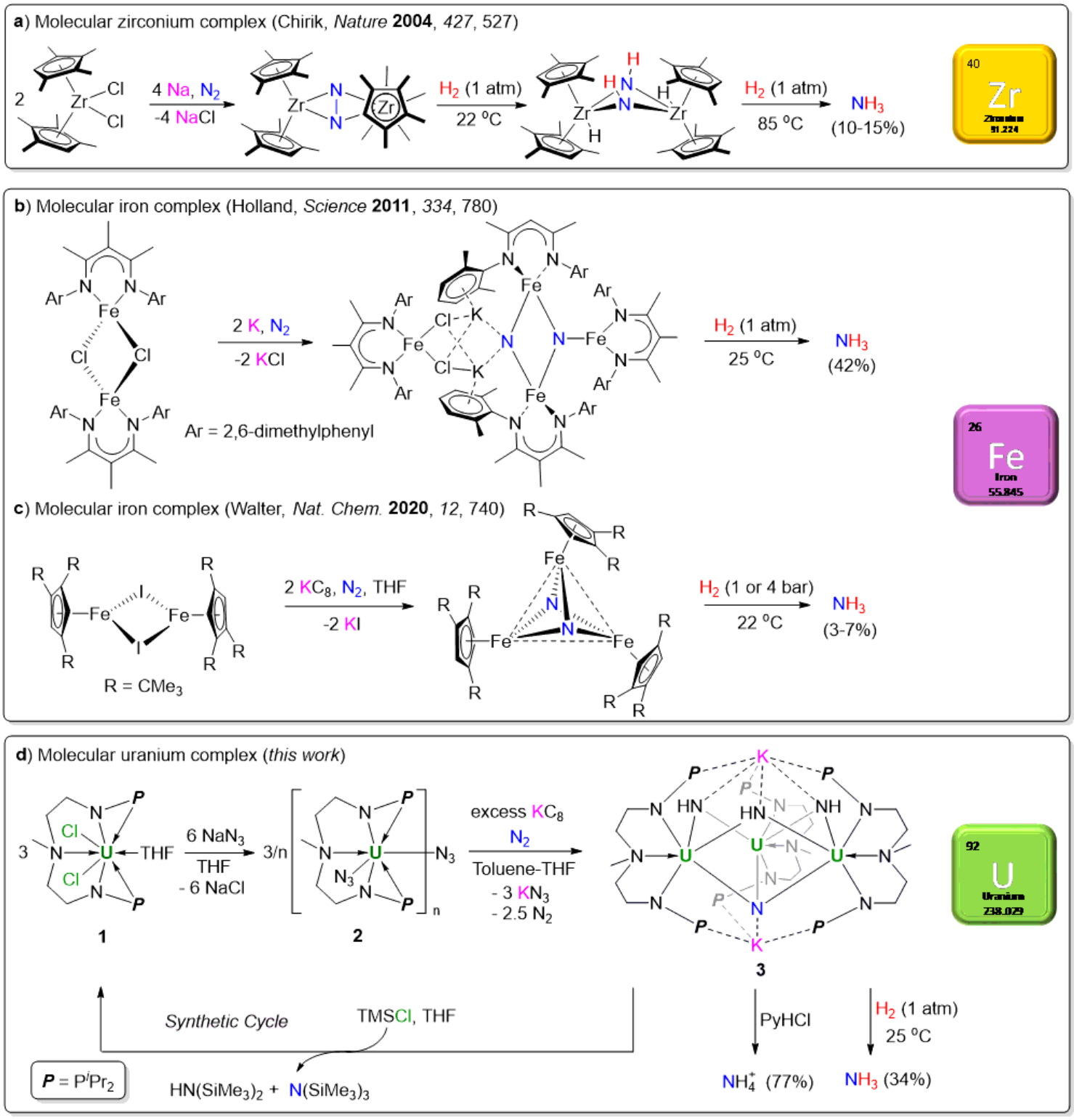

Figure 1

NH3 formation from N2 and H2 promoted by molecular complexes. a) Hydrogenation and cleavage of N2 to NH3 with a Zr complex.12 b,c) N2 reduction and hydrogenation to NH3 with Fe complexes.16,29 d) N2 cleavage and hydrogenation to NH3 with a U complex (this work). N2 activation or cleavage occurs under reducing conditions with Na, K, or KC8. The N atoms originating from N2 are shown in blue.

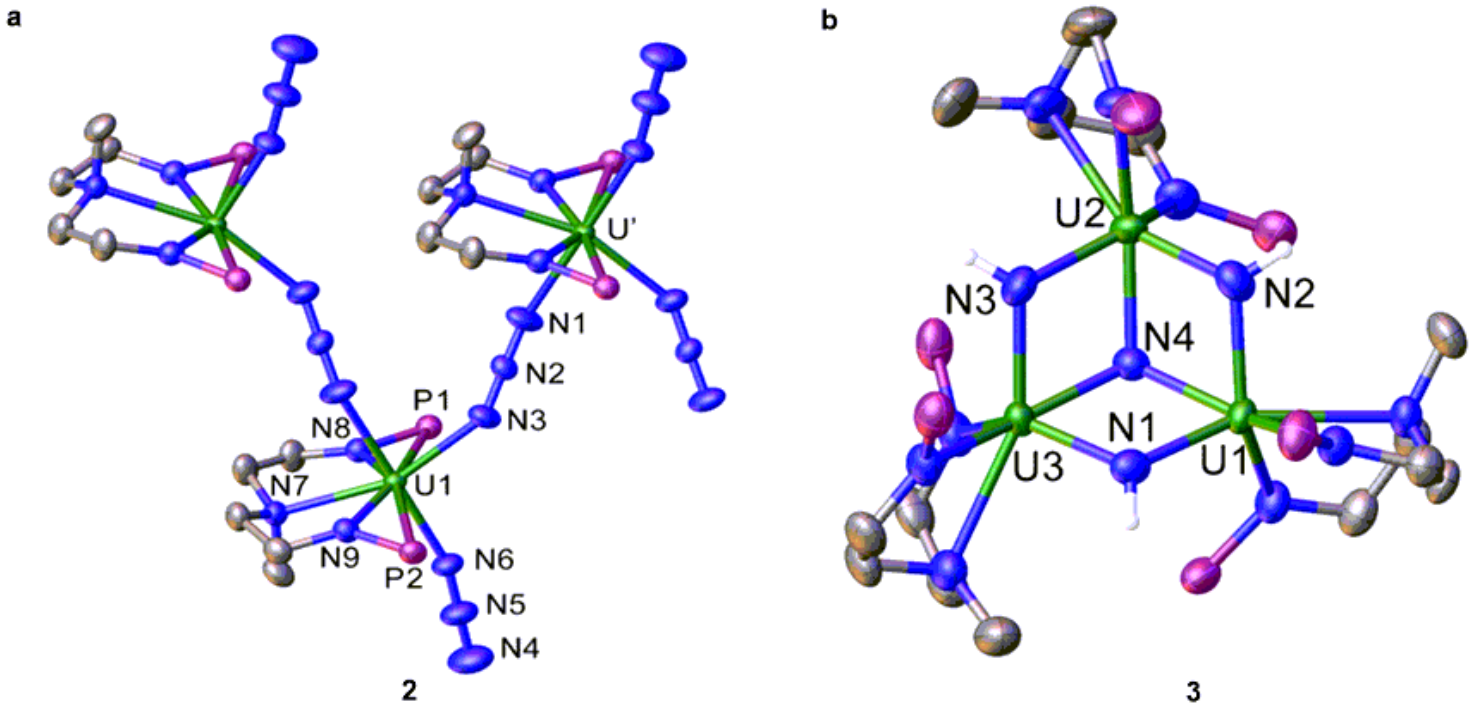

Figure 2

Solid-state structures of complexes 2 (a) and 3 (b) by X-ray crystallography with 50% probability ellipsoids. Solvent molecules, H atoms (except for the NH protons), isopropyl moieties in PiPr2, and two K+ counter ions in complex 3 are omitted for clarity. Uranium, green; phosphorus, violet red; nitrogen, blue; and carbon, grey.

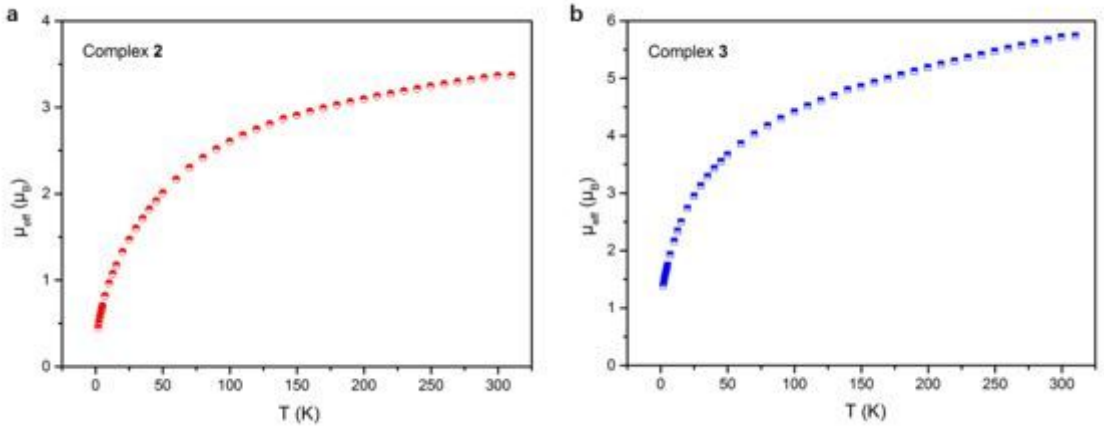

Figure 3

Variable-temperature effective magnetic moment data of complexes 2 (a) and 3 (b).

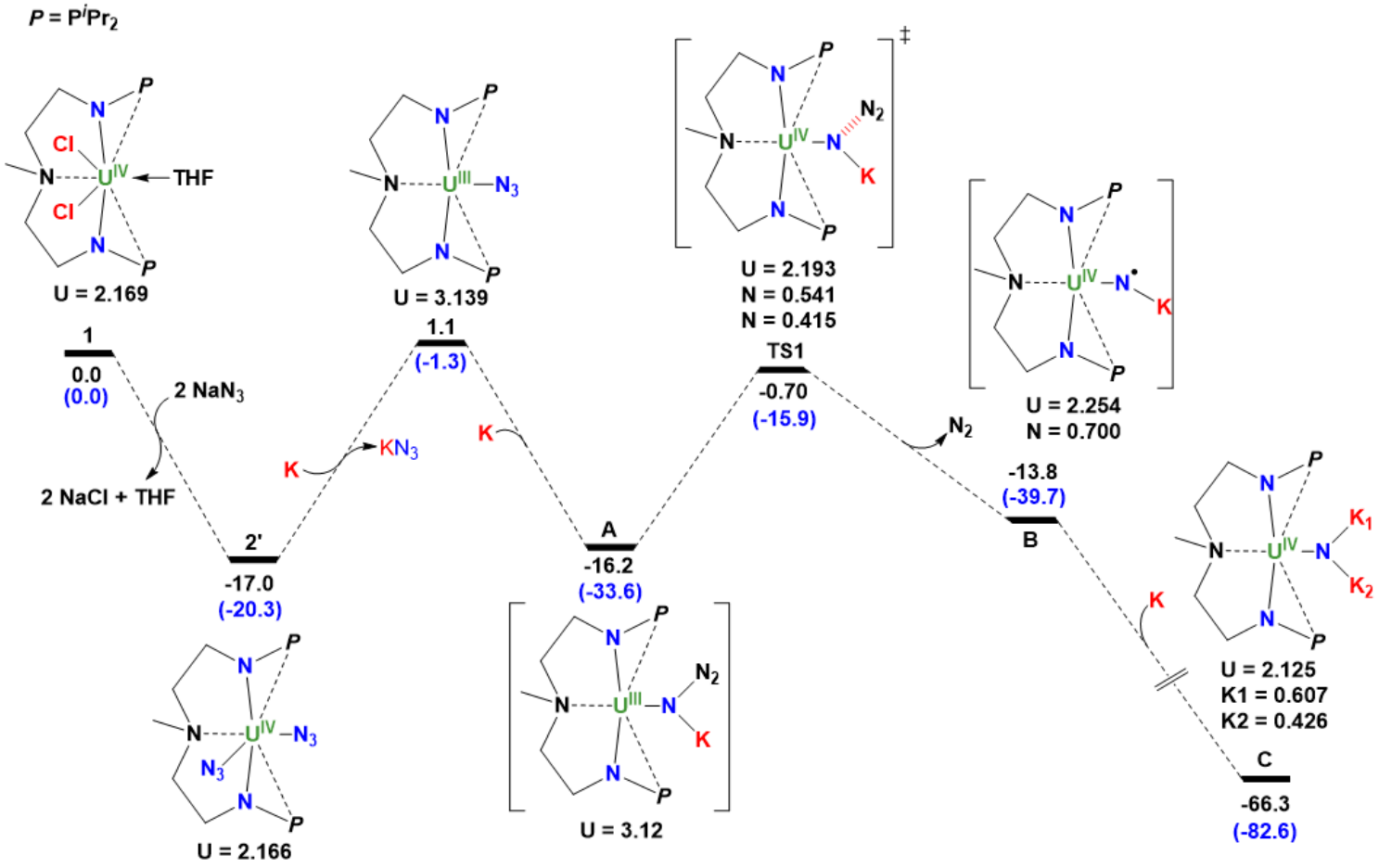

Figure 4

Computed enthalpy profile (in kcal mol-1) for the reduction of 2’ to a dianionic uranium-nitride intermediate C. Gibbs free energies are given in parentheses.

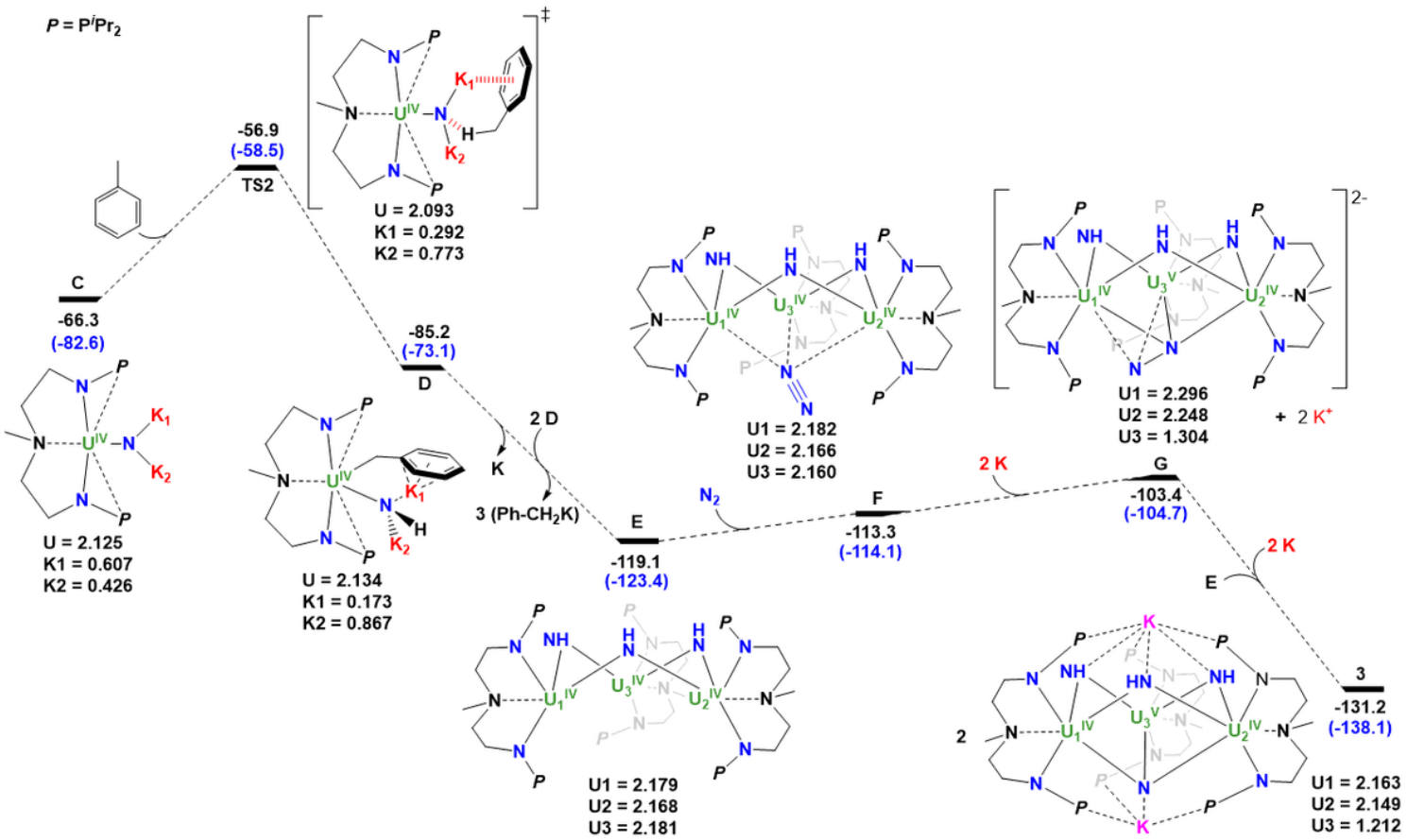

Figure 5

Computed enthalpy profile (in kcal mol-1) for the formation of 3 from the uranium-nitride C. Gibbs free energies are given in parentheses.

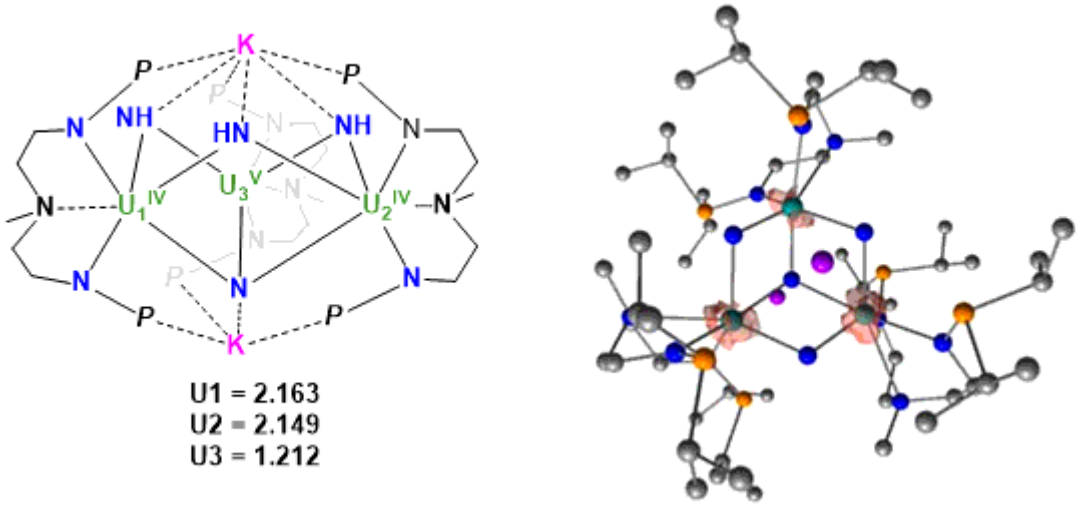

Figure 6

Unpaired spin density plot of complex 3.

Supplementary Files

This is a list of supplementary files associated with this preprint. Click to download.

- 2.cif
- checkcif3preparedunderAr.pdf
- 3preparedunderAr.cif
- 2checkcif.pdf
- checkcif3preparedunderN2.pdf
- SupplementaryInformation.pdf
- 3preparedunderN2.cif